CD47 in the tumor microenvironment and CD47 antibody blockade regulate natural killer cell recruitment and activation

Running title: CD47 regulates NK cell-mediated tumor immunity

Pulak Ranjan Nath[1*§], Dipasmita Pal-Nath[1], Ajeet Mandal[2], Maggie Cam[3] Anthony L. Schwartz[1], and David D. Roberts[1*]

[1]Laboratory of Pathology, Center for Cancer Research, National Cancer Institute, National Institutes of Health, Bethesda, MD, USA

[2]Human Brain Collection Core, National Institute of Mental Health, National Institutes of Health, Bethesda, MD, USA

[3]CCR Collaborative Bioinformatics Resource, Office of Science and Technology Resources, National Cancer Institute and Leidos Biomedical Research, Inc., National Institutes of Health, Bethesda, MD, USA

*Correspondence
Dr. David D. Roberts
droberts@mail.nih.gov

Dr. Pulak R. Nath
hellopran2000@gmail.com

§ Current address: The Jackson Laboratory for Genomic Medicine, Farmington, CT, USA

Supplementary Methods

Reagents:

DAPI (Cat#D9542), Rat serum (Cat#R9759) and Rabbit serum (Cat#R9133) were purchased from Sigma-Aldrich. Aqua live/dead was from ThermoFisher Scientific (Cat#L3495), UV Zombie from BioLegend (Cat#423107) and ACK lysis buffer was bought from Lonza (Cat#10-548E).

Apoptosis analysis:

Cells were stained with annexin V according to the manufacturer instructions (BD Biosciences). Cells were washed in PBS and resuspended in 1× annexin binding buffer containing allophycocyanin-conjugated annexin V. After 15 min of incubation at room temperature, cells were diluted in 1× annexin V binding buffer and analyzed by flow cytometry.

Tumor processing:

Tumors were cut into small pieces and enzymatically dissociated with Collagenase/Dispase (Roche, Cat# 269638, final concentration 1 mg/ml) and DNase 1 (Sigma, Cat# D4527, final concentration 100 µg/ml). The suspension was centrifuged with 50xg for 5 minutes to separate tissue debris, and supernatant cell suspension was filtered through a 70 µm strainer followed by centrifugation with 330xg for 5 minutes. RBC were lysed using ACK buffer, and cells were suspended in FACS buffer followed by staining or sorting.

Seahorse mitochondrial stress analysis:

Briefly, NK cells from spleens of WT and *Cd47*$^{-/-}$ littermate mice were isolated and plated at $0.75x10^6$ cells/well in 24-well plates (Seahorse Bioscience) into XF Base Medium (Seahorse

Bioscience) with added 10 mM glucose, 1 mM sodium pyruvate and 2 mM L-glutamine, pH 7.4. Subsequently, analyses of OCR and EACR were performed in a Seahorse analyzer. The OCR and EACR values were obtained during baseline (prior to addition of any Mito Stress Test substances) and after the addition of 0.5 μM oligomycin, 1 μM FCCP and 0.5 μM rotenone + 0.5 μM antimycin A. Background values from media only were subtracted, and data were corrected by subtracting non-mitochondrial respiration (measured after the injection of rotenone + antimycin A) from all measured OCR values.

Reactive oxygen species (ROS) assay:

Briefly, isolated NK cells from WT and littermate *Cd47*$^{-/-}$ mice were subjected to Seahorse Mito stress analysis with ATP synthase inhibitor oligomycin (0.5 μM), mitochondrial uncoupler carbonyl cyanide 4-(trifluoromethoxy) phenylhydrazone (FCCP, 1 μM) and complex I + II inhibitors rotenone (0.5 μM) + antimycin A (0.5 μM). Cells were then incubated with the ROS detection reagent, and the red fluorescence intensity was measured on a flow cytometer.

Flow cytometry and cell sorting:

Antibodies were directly conjugated to Brilliant Ultraviolet (BUV)395, Brilliant Violet (BV)786, BV711, BV650, BV605, Pacific Blue (PB), fluorescein isothiocyanate (FITC), phycoerythrin (PE), PE-Cy5.5, PE-Texas Red, peridinin-chlorophyll-protein complex (PerCP)-Cy5.5, PE-Cy7, allophycocyanin (APC), APC-Alexa 700, or biotin. Biotinylated antibodies were revealed with Streptavidin APCeFluor780. Cells were resuspended in FACS buffer (1% BSA+0.01% NaN_3 in PBS1x, filtered) and incubated with rat plus rabbit serum followed by incubation with antibody cocktail against surface molecules. Dead cells were excluded through 4,6 diamidino-2-phenylindole (DAPI) uptake or Aqua live/dead staining. Doublets were excluded through

forward scatter–height by forward scatter–width and side scatter–height by side scatter–width parameters. Data were analyzed using FlowJo (Tree Star).

RNA-seq library construction and Illumina sequencing:

During RNA isolation, DNase treatment was additionally performed using the RNase-free DNase set (Qiagen). RNA quality was reported as a score from 1 to 10, and samples falling below the threshold of 8.0 were omitted from the study. cDNA library preparation involves the removal of ribosomal RNA (rRNA) using biotinylated, target-specific oligos combined with Ribo-Zero rRNA removal beads. The RNA is fragmented into small pieces and the cleaved RNA fragments are copied into first strand cDNA using reverse transcriptase and random primers, followed by second strand cDNA synthesis using DNA Polymerase I and RNase H. The resulting double-strand cDNA is used as the input to a standard Illumina library prep with end-repair, adapter ligation and PCR amplification being performed to give you a library that is ready to go to the sequencer. The final purified product is then quantitated by qPCR before cluster generation and sequencing. The samples have 99 to 148 million pass filter reads with a base call quality of above 92% of bases with Q30 and above.

The sequencing reads were trimmed adapters and low-quality bases using Trimmomatic (version 0.30), the trimmed reads were mapped to mouse reference genome (GRCm38/mm10) and Gencode annotation M9 using STAR (version 2.5) with two-pass alignment option. RSEM (version 1.2.22) was used for transcript quantification.

RNA-seq data processing and analysis:

To remove the adapter sequences cutadapt/1.14 was used followed by fastQ Screen v0.9.3 to screen the library for its composition. For quality control the tool fastqc/0.11.5 was used and the

spliced transcripts alignment to a reference genome and counting the number of reads per gene was performed by STAR/2.5.2b. The mapped reads in the genomic features were counted by subread/1.5.1 and the distribution of these reads was calculated by rseqc/2.6.4 along with the estimation of strandness of the reads. The library complexity was estimated by preseq/2.0.3. To mark duplicate reads and estimate the gene coverage the program picard/1.119 and for the overall statistics of input datasets samtools/1.5 was used. For differential expression analysis, the low abundant gene threshold was set to include genes with ≥ 0.5 counts per million (CPM) in at least ≥ 4 samples. In order to generate the gene lists based on different contrast the R Bioconductor package DESeq2 was used. PCA analysis was performed using Partek Genomics Suite (v 6.5) and Gene Set Enrichment Analysis (GSEA) performed using software provided by the Broad Institute.

CD47 correlation with gene expression and survival in human cancers

The Cancer Genome Atlas (TCGA) tumor RNAseq expression data from 469 melanoma patients in the Skin Cutaneous Melanoma TCGA Provisional dataset were analyzed using cBioPortal tools as described (1,2). Coexpression analysis was performed to identify genes that correlated with elevated mRNA expression of CD47. To assess correlation between CD47 mRNA expression and survival, tumors were grouped into high and low CD47 expression using the mean expression or >1 SD above or below the mean as cutoffs. Correlation of overall or progression-free survival for IL-15 or an early NK activation gene signature used mean expression as the cutoff. TCGA Provisional datasets for other cancers that contained sufficient RNAseq expression and survival data were analyzed similarly. Kaplan-Meier survival curves were prepared in cBioPortal to determine logrank test p-values.

References

1. Gao J, Aksoy BA, Dogrusoz U, Dresdner G, Gross B, Sumer SO, et al. Integrative analysis of complex cancer genomics and clinical profiles using the cBioPortal. Sci Signal. 2013;6(269):pl1.

2. Cerami E, Gao J, Dogrusoz U, Gross BE, Sumer SO, Aksoy BA, et al. The cBio cancer genomics portal: an open platform for exploring multidimensional cancer genomics data. Cancer Discov. 2012;2(5):401-4.

Supplemental Tables:

Supplemental Table S1. (Excel file) Gene list of DEG normalized and log_2 transformed expression values of significantly differentially expressed genes within the following contrasts: *Cd47*$^{-/-}$ Uninfected vs WT Uninfected, WT Tumor bearing vs WT Uninfected, *Cd47*$^{-/-}$ Tumor bearing vs *Cd47*$^{-/-}$ Uninfected and *Cd47*$^{-/-}$ Tumor bearing vs WT Tumor bearing.

Supplemental Table S2. (Excel File) GSEA gene ranklist of NK cell genes from WT and *Cd47*$^{-/-}$ uninfected and B16F10 tumor-bearing mice within the following signatures: Naïve, Early Effector, Sustained Effector, Late Effector, Memory, Interferon, Cell Cycle & Proliferation and Apoptosis & Cell Death.

Supplemental Table S3. Primers used for qRT-PCR analysis of gene expression.

Supplemental Table S4. Antibody list.

Supplemental Table S3. Primers used for qRT-PCR analysis of gene expression.

Gene	Forward primer	Reverse primer
beta-Actin	5'-ATGGAGGGGAATACAGCCC-3'	5'-TTCTTTGCAGCTCCTTCGTT-3'
Cd69	5'- ACGCTCTTGTTCTGAAGATGCTGC-3'	5'- TCCAATGTTCCAGTTCACCA-3'
Cish	5'- CGACTACCTCCGACAGTACC-3'	5'- TGTGACAATCCCTCCTCCAC-3'
Gapdh	5'-TGTGTCCGTCGTGGATCTGA-3'	5'-CCTGCTTCACCACCTTCTTGAT-3'
Gzmb	5'-CATGTAGGGTCGAGAGTGGG-3'	5'-CCTCCTGCTACTGCTGACCT-3'
Ifng	5'-TGAGCTCATTGAATGCTTGG-3'	5'-ACAGCAAGGCGAAAAAGGAT-3'
Klrc1	5'- CGAAGGATTCCAGTCCATGA-3'	5'- GGTGTCCTGCATTTCCAAAA-3'
Klrc2	5'- CTCAAACTCAATGACAGCCTTG-3'	5'-TGAAACACCTGCACTGGAAG-3'
Klrk1	5'- GTGGTTGCTGGGATTTGAAC-3'	5'- TGCCTCTTAAGAATGCACCC-3'
Lag3	5'- CTGGGACTGCTTTGGGAAG-3'	5'- GGTTGATGTTGCCAGATAACCC-3'
Mcam	5'- CCCAAACTGGTGTGCGTCTT-3'	5'-GGAAAATCAGTATCTGCCTCTCC-3'
Mmp9	5'- GCAGAGGCATACTTGTACCG-3'	5'- TGATGTTATGATGGTCCCACTTG-3'
Ncr1	5'-GGCTGCTGTTCTCAACACCT-3'	5'- GGCTCACAGAGGGACATACA-3'

Supplemental Table S4. Antibody list.

Antibodies	Clone	Origin
Lin cocktail:		
B220	RA3-6B2	eBioscience
CD19	eBioD3	eBioscience
Gr1	RB6-8C5	eBioscience
CD11c	N418	eBioscience
Ter119	TER-119	eBioscience
Cell surface:		
CD45.2	104	eBioscience
CD4	RM4-5	eBioscience
CD8	53-6.7	eBioscience
CD3	145-2C11	BD Pharmingen
NK1.1	PK136	eBioscience
NKp46	29A1.4	eBioscience
CD122	TM-b1	eBioscience
CD127	A7R34	eBioscience
CD11b	ICRF44	BioLegend
CD11c	HL3	BioLegend
CD69	H1.2F3	BioLegend
CD44	IM7	eBioscience
CD62L	MEL-14	BioLegend
KLRG1	2F1/KLRG1	BioLegend
PD-1	29F.1A12	BioLegend
PD-L1	10F.9G2	BioLegend
TIGIT	IG9	BioLegend
CD39	A1	BioLegend
CD47	miap301	eBioscience
Intracellular:		
TNF-α	MP6-XT22	BioLegend
Ki-67	SolA15, B56	BD Pharmingen
Eomes	Dan11mag	eBioscience
T-bet	eBio4B10	eBioscience
IL-2	JES6-5H4	eBioscience
IFN-γ	XMG1.2	eBioscience
Granzyme B	NGZB, GB11	BioLegend

Supplemental Figures:

A

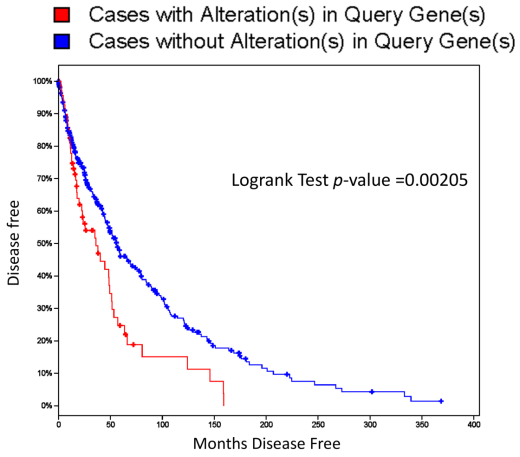

DFS/PFS melanoma	#total cases	#cases relapsed	median months disease free
Cases with CD47 >1 SD below the mean	**70**	**47**	**35.87**
Cases without Alterations in CD47	**332**	**212**	**55.85**

B

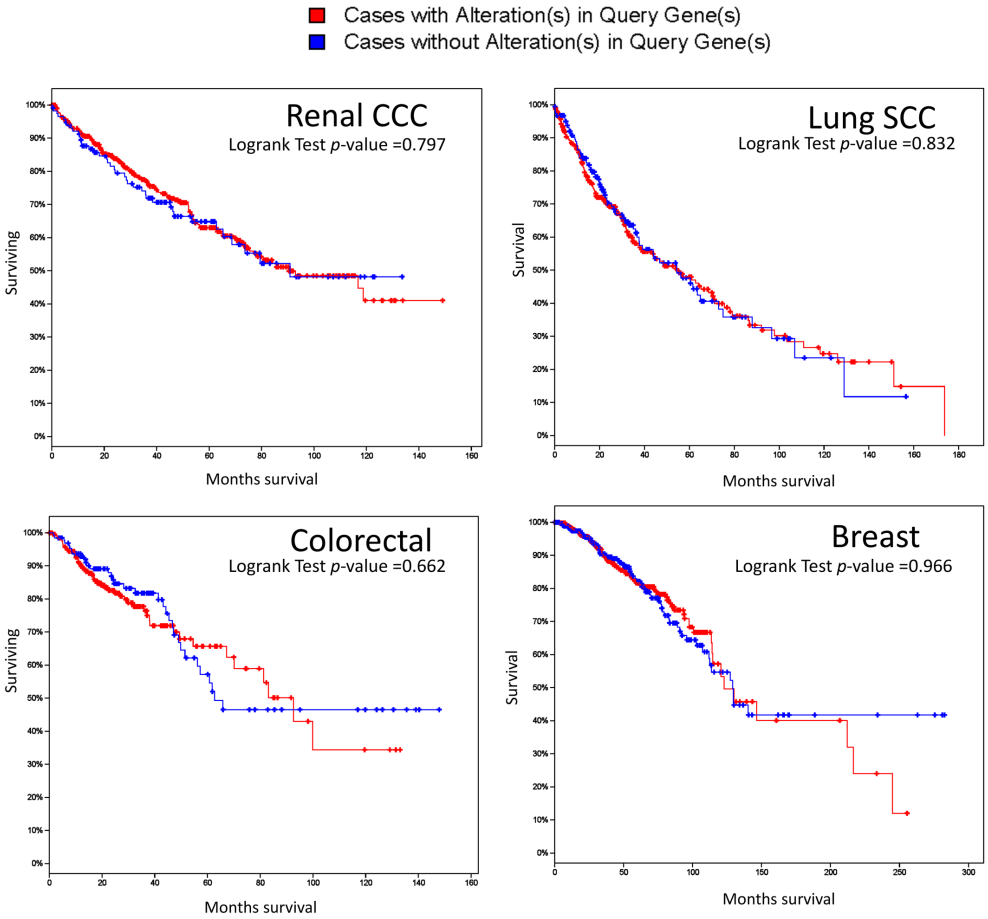

c

Gene	NK signature*	breast	liver	glioma	Renal CC	Renal papillary	Lung adeno	Lung SCC	Colorectal	Uterine endometrial
IFIH1	Early NK effector signature	0.37, 0.40§	NS	NS	NS	NS	NS	0.30, 0.38	NS	NS
TBX21 (TBET)	Early NK effector signature	NS	NS	NS	NS	NS	NS	NS	NS	NS
STAT1	Early NK effector signature	0.30, 0.34	NS	NS	0.40, 0.35	NS	NS	NS	NS	NS
IFNG	Early NK effector signature	NS	NS	NS	0.38, 0.32	NS	NS	NS	NS	NS
GBP4	Early NK effector signature	NS	NS	NS	NS	0.33, 0.43	NS	NS	NS	NS
IL2RA (CD25)	Early NK effector signature	NS	NS	NS	NS	0.38, 0.39	NS	NS	NS	NS
KLRG1	Late NK effector signature	NS	NS	NS	NS	NS	NS	NS	NS	NS
NLRC5	NK sustained effector signature	NS	NS	NS	NS	NS	NS	NS	NS	NS
GZMA	Naïve NK signature	NS	NS	NS	NS	NS	NS	NS	NS	NS
GZMB	Naïve NK signature	NS	NS	NS	NS	NS	NS	NS	NS	NS
GZMK	NK effector	NS	NS	NS	NS	NS	NS	NS	NS	NS
NCR1 (NKp46)	Naïve NK signature	NS	NS	NS	NS	NS	NS	NS	NS	NS
KLRB1 (NK1.1)	Naïve NK signature	NS	NS	NS	NS	NS	NS	NS	NS	NS
KLRC1	NK receptor	NS	NS	NS	NS	NS	NS	NS	NS	NS
KLRK1 (NKG2D)	NK receptor	NS	NS	NS	NS	NS	NS	NS	NS	NS
KLRD1 (CD94)	NK receptor	NS	NS	NS	NS	0.34, 0.35	NS	NS	NS	NS

D

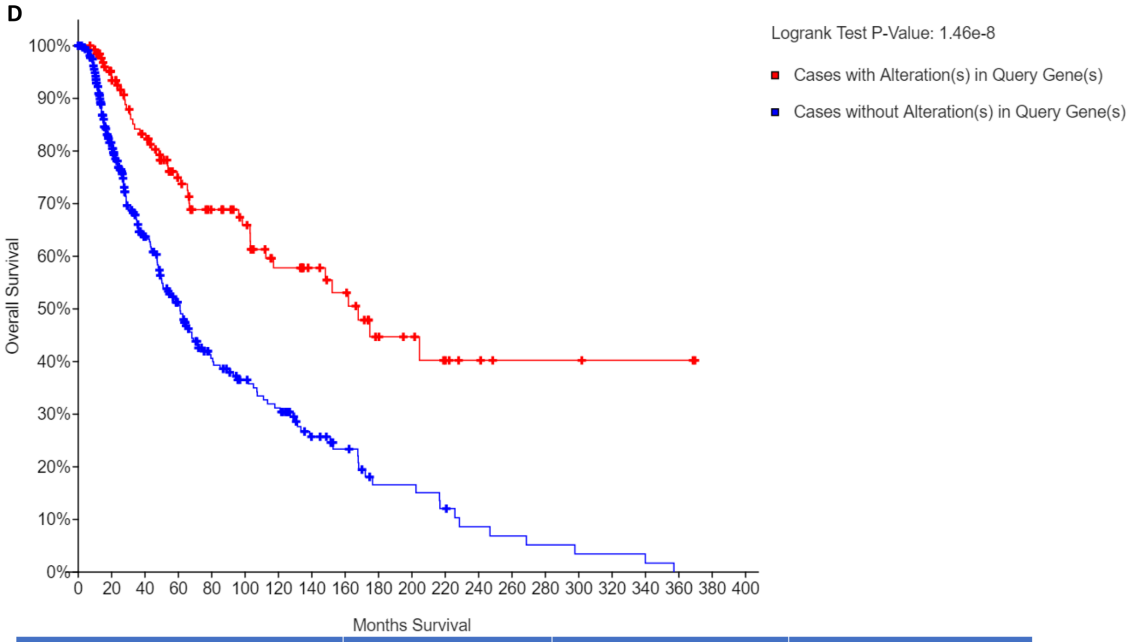

	Number of Cases, Total	Number of Cases, Deceased	Median Months Survival
Cases with IL-15>mean	**132**	**45**	**167.87**
Cases with IL-15<mean	**328**	**175**	**61.1**

E

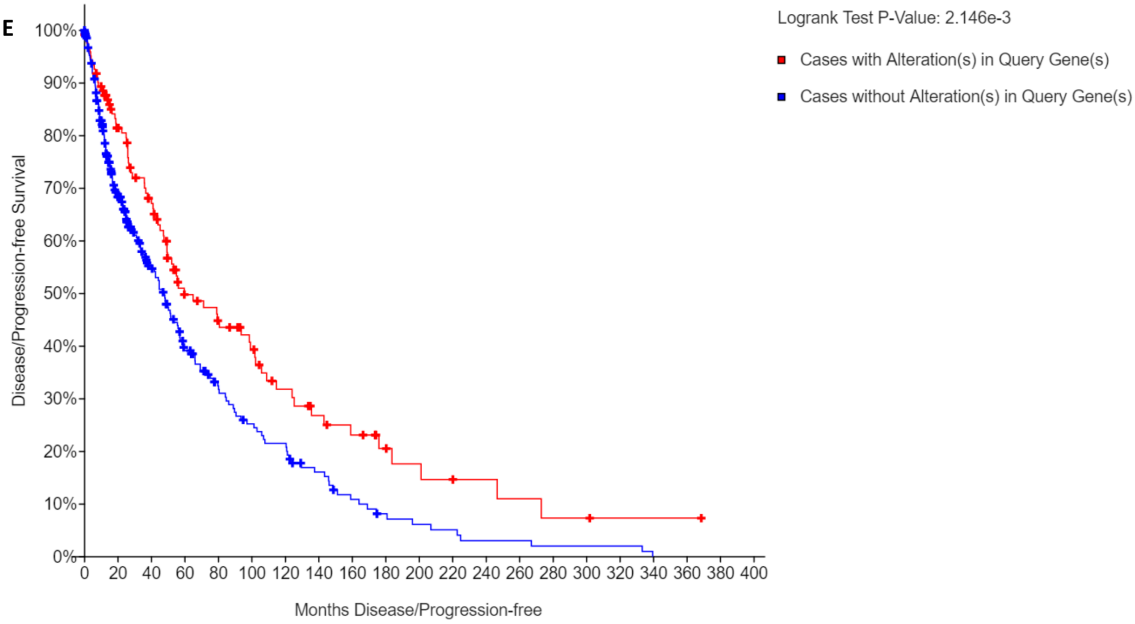

	Number of Cases, Total	Number of Cases, Relapsed/Progressed	Median Months Disease-free
Cases with IL-15>mean	**124**	**76**	**59.59**
Cases with IL-15<mean	**279**	**184**	**47.6**

Supplementary Figure S1. (A) Dose-dependent correlation between CD47 mRNA expression and disease free/progression free survival in TCGA melanoma data. **(B)** Lack of correlation of overall survival with mRNA expression for 6 NK cell early activation genes > (red) versus < mean (blue) for the indicated cancers. **(C)** Analysis of TCGA RNAseq data for co-expression correlations between CD47 mRNA and naïve or activated NK signature genes as defined in Bezman et al Nature Immunol, 2012. Pearson and Spearman's correlations were determined using cBioPortal tools using TCGA RNAseq data for the indicated cancer types. §Pearson score, Spearman score, NS = correlations <0.2. **(D,E)** Elevated IL-15 expression (>mean) is associated with improved survival in TCGA melanoma data. (n = 469 patients)

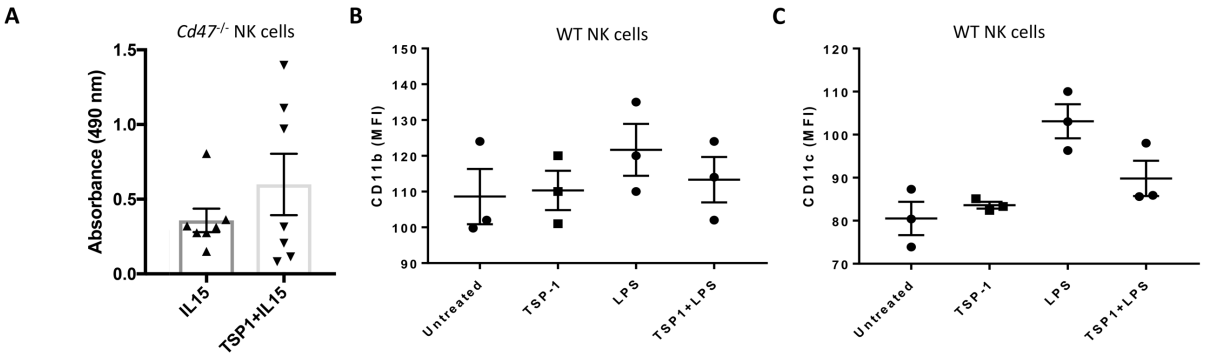

Supplement Figure S2. Thrombospondin-1 does not inhibit *Cd47*$^{-/-}$ NK cell proliferation
(A) NK cells were isolated from spleens of *Cd47*$^{-/-}$ mice by MACS NK isolation kit.
Cells were cultured in serum free RPMI with IL15 and with/out thrombospondin-1 (2 nM) and MTS absorbance was measured after 24 hours.
Isolated WT NK cells were divided into 4 groups and cultured in serum free RPMI with thrombospondin-1 (2 nM), LPS (1 µg/ml) or both. Cell surface protein levels of Cd11b **(B)** and **(C)** CD11c were measured by flow cytometry within 24 hours of treatment, n= 3.

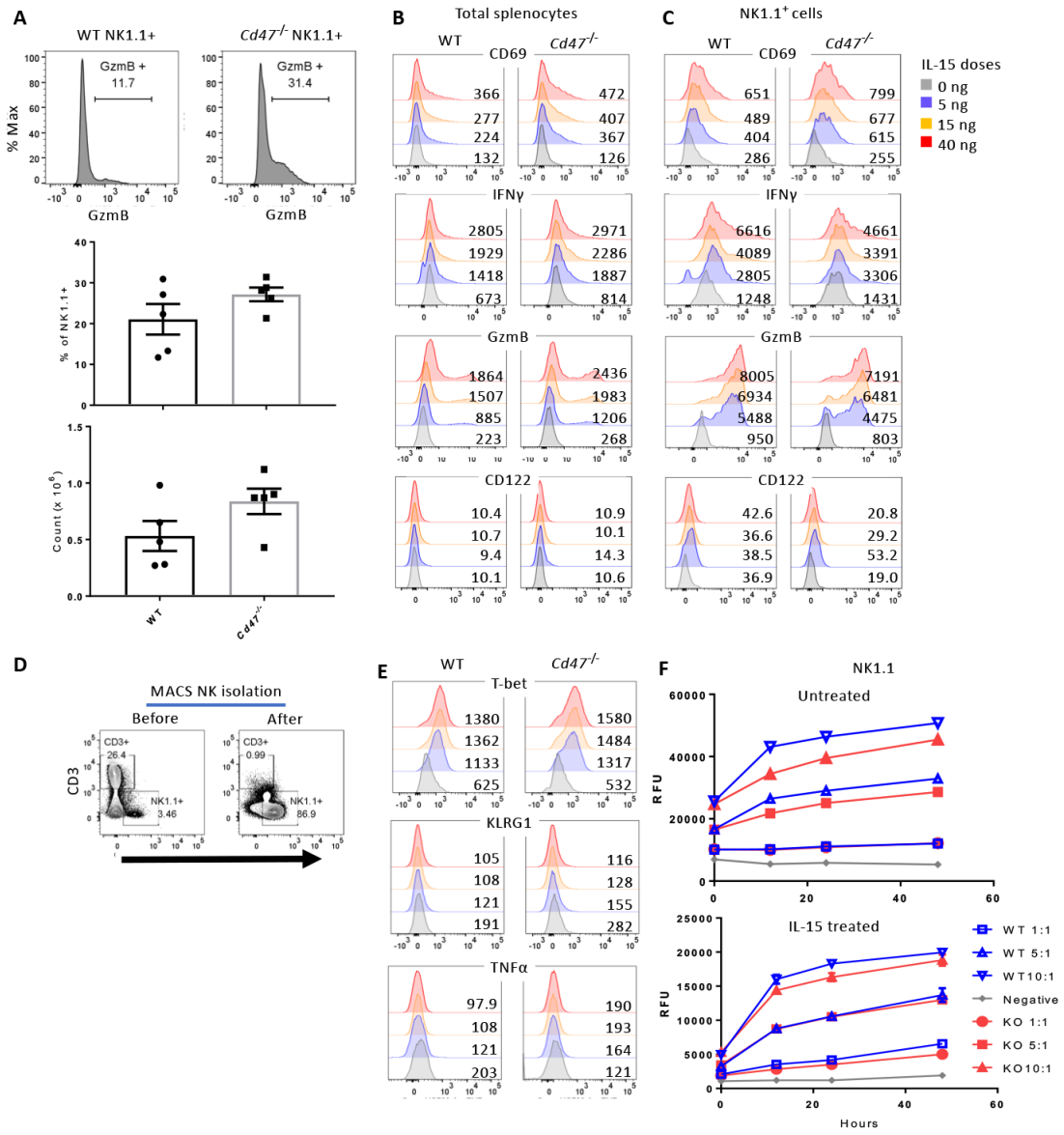

Supplementary Figure S3. (A) Splenocytes of WT and *Cd47*$^{-/-}$ littermate mice were FcR-blocked and stained for surface proteins. Cells were then fixed, permeabilized and i.c. stained for granzyme B (GzmB). Representative plots, frequency and count of GzmB^{+} cells within the live CD3^{-}CD4^{-}CD8^{-}NK1.1^{+} population. n=5. **(B-C)** Pooled splenocytes of 3 WT and 3 *Cd47*$^{-/-}$ littermate mice were cultured untreated or with IL-15 (5, 15 and 40 ng/ml) for 24 hrs with Golgi-stop. Cells were FcR blocked, stained for surface proteins followed by i.c. staining. Histograms show expression of CD69, IFNγ, GzmB and CD122 in splenocytes **(B)** and within the NK1.1^{+} papulation **(C)**. Values on the plot are MFI of indicated proteins. **(D)** Representative plots show enrichment of NK cells by MACS isolation kit. **(E)** NK cells were isolated from spleens of WT and *Cd47*$^{-/-}$ littermate mice and cultured with IL-15 (5, 15 and 40 ng/ml) for 24 hrs and stained for cell surface KLRG1, and i.c. T-bet and TNFα. **(F)** Isolated NK cells were untreated or treated with IL-15 (5 ng/ml for 24 hrs) and co-cultured with B16F10 with E:T ratio as 1:1, 5:1 and 10:1. Cell cytotoxicity was measured by Cell-Tox-Green at indicated hours.

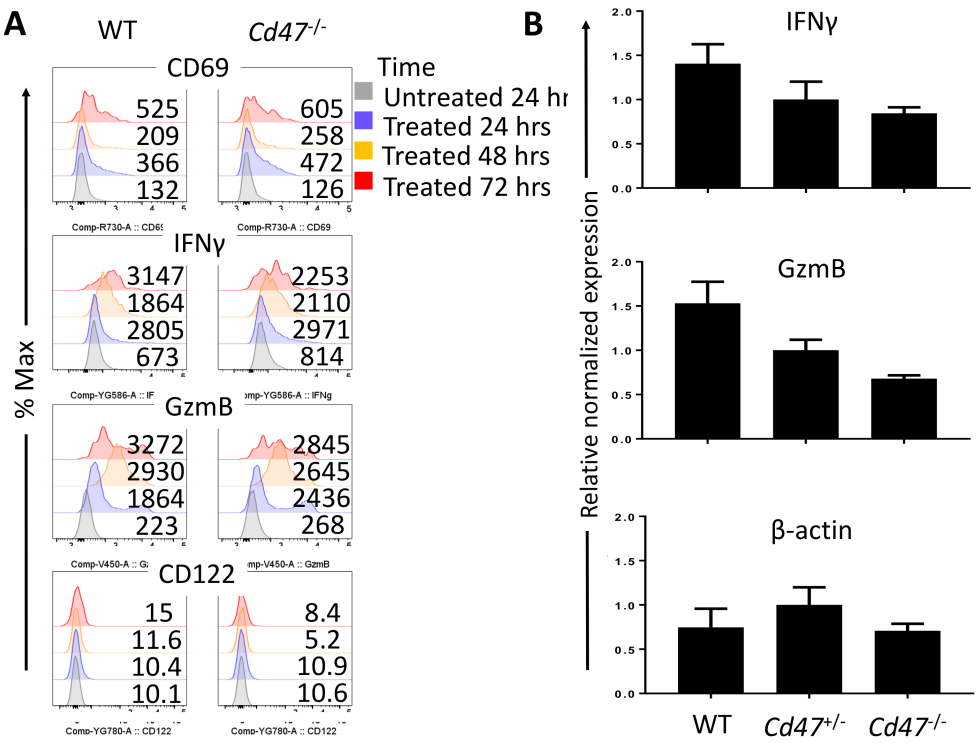

Supplementary Figure S4. (A) Single cell suspensions from splenocytes of WT and *Cd47*$^{-/-}$ littermate mice were treated with IL-15 (5, 15 and 40 ng/ml) for the indicated hours in complete RPMI (10% FCS). Golgi-stop was added at the last 4 hrs of incubation. FcR was blocked and cells were stained for Aqua live/dead, CD69 and CD122. Cells were then fixed, permeabilized and i.c. stained for IFNγ and granzyme B. Histograms show expression of CD69, IFNγ, granzyme B and CD122 in the cultured spleenocytes. Values on the plot are MFI of indicated protein in live cells. **(B)** NK cells were negatively enriched from spleens of WT, *Cd47*$^{+/-}$ and *Cd47*$^{-/-}$ littermate mice using MACS kit. Cells were then cultured with IL-15 (40 ng/ml) in complete RPMI for 72 hrs. Bar diagrams show mRNA expression of *Ifng, Gzmb* and *β-Actin* genes in the indicated genotypes. *Gapdh* is used as internal control. n=3.


A
Cd47
n= 5
Il-2ra
Gzmc
Mki67
Mapk13
Cxcr1
Ifna2
Jun
Ifna13
Ifna4
-log10 (p value)
Fold change
B
group
Naive
EarlyEffector
Memory
SustainedEffector
Proliferation
Interferon
NA
WT
Cd47-/-
C
Regulation
Top downregulation
Top upregulation
Immune response
surface receptor signaling pathway
Regulation of cytokine production
Signal transduction
Innate immune response
ive regulation of metabolic process
Ion transport
Regulation of lipid storage
Regulation of response to stress
Anion transport
Chemotaxis
toll-like receptor signaling pathway
Response to oxidative stress
ive regulation of T cell proliferation
on of interferon-gamma production
Regulation of mitochondrion organization
Positive regulation of mitochondrial proteins
mTOR signalling
p53 pathway
Pathways in cancer
TCR signaling in naive CD8+ T cells
Wnt signaling pathway
Diseases of signal transduction
MAPK signaling pathway
Natural killer cell mediated cytotoxicity
Signaling by EGFR
Integrin-mediated Cell Adhesion
DAP12 signaling
Fc epsilon receptor (FCERI) signaling
Golgi membrane
log10(pval)
-log10(pval)
D
positive regulation of inflammatory response
positive regulation of defense response
immune response-activating signal transduction
phagocytosis
activation of immune response
complement activation
phagocytosis
activation of immune response
immune response-activating signal transduction
positive regulation of inflammatory response
positive regulation of defense response
Significance color code
No. of mapped genes

Supplementary Figure S5. CD47 regulates effector gene expression in naive NK cells. (A) Volcano plot shows that many genes, including the indicated *Il-2ra*, *Ifna2*, *Ifna4*, *Ifna13*, *Gzmc*, *Mapk13*, *Jun* and *Cxcr1* are significantly upregulated in naïve *Cd47*$^{-/-}$ compared to naïve WT NK cells. **(B)** Heatmap shows unsupervised expression of NK naïve, early effector, sustained effector, memory, proliferation and interferon signature genes in naïve WT and *Cd47*$^{-/-}$ NK cells, n=5. **(C)** Waterfall plot shows significant up/down-regulation of distinct pathways in *Cd47*$^{-/-}$ NK cells than in WT NK cells. **(D)** The inflammatory response pathway was found to be significantly upregulated (p=2.10e^{-23}, Activation Z score 5.361) in naïve *Cd47*$^{-/-}$ NK cells than in naïve WT NK cells. Cytoscape functional and molecular interaction network shows comparison of expression of 213 molecules within the inflammatory response pathway.

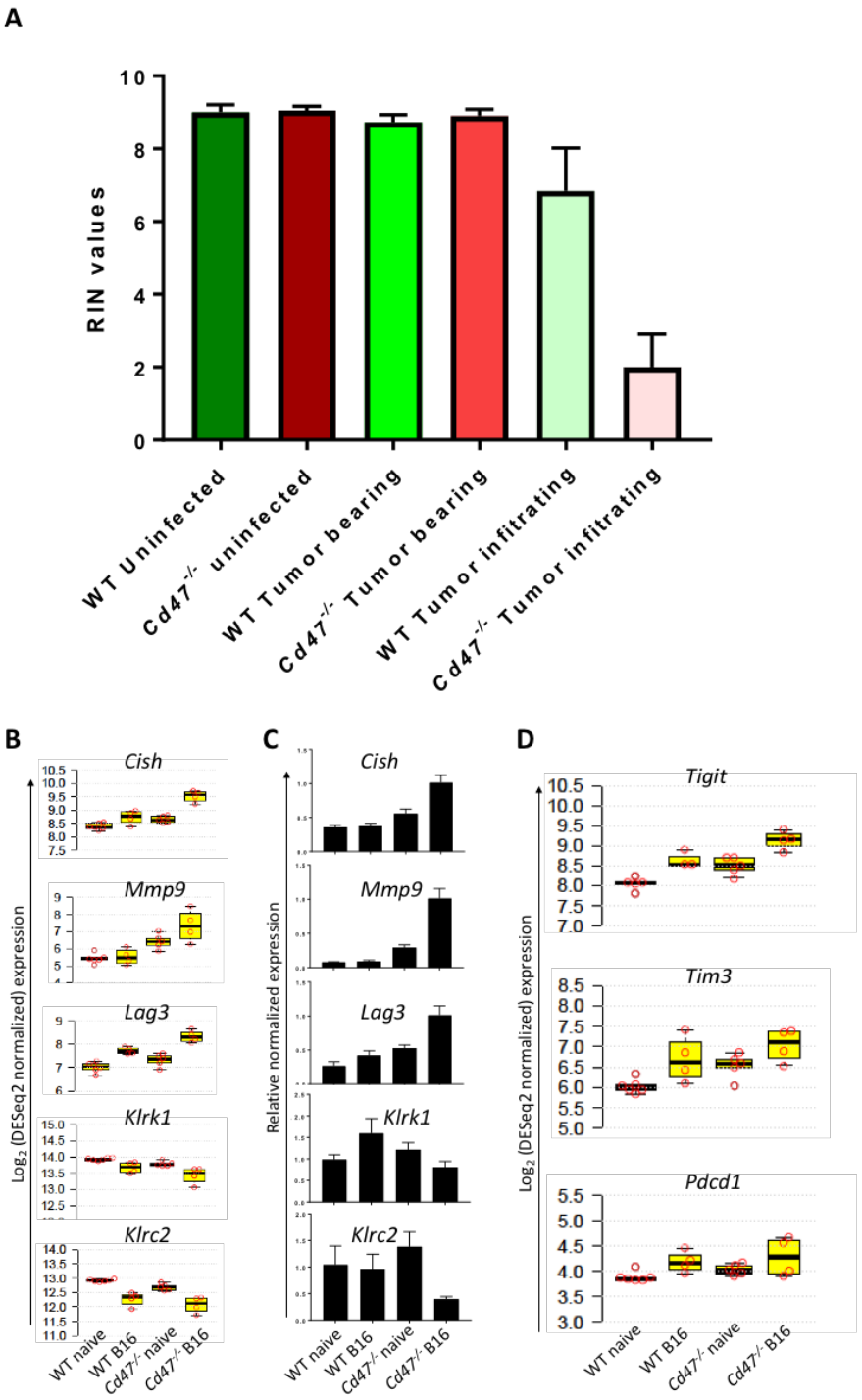

Supplementary Figure S6. (A) RIN values of total RNA extracted from NK cells from spleens of WT and *Cd47*$^{-/-}$ naïve and tumor baring mice, and also from tumor infiltrating NK cells, n ≥ 4. **(B)** Boxplots show log2 expression of *Cish*, *Mmp9*, *Lag3*, *Klrk1*, and *Klrc2* genes in WT and *Cd47*$^{-/-}$ naïve NK cells and their corresponding **(C)** ΔCt values of gene expression calculated after normalizing to *β-actin* expression by qRT-PCR. **(D)** Boxplots show log2 expression of *Tigit*, *Tim3* and *Pdcd1* genes in WT and *Cd47*$^{-/-}$ naïve NK cells.

Supplementary Figure S7. Waterfall plot shows top up- and down-regulated pathways in *Cd47*$^{-/-}$ NK cells from tumor bearing mice.